ELSEVIER

J. Non-Newtonian Fluid Mech. 114 (2003) 185–195

Journal of Non-Newtonian Fluid Mechanics

www.elsevier.com/locate/jnnfm

Planar contraction flow with a slip boundary condition

Yogesh M. Joshi, Morton M. Denn*

Benjamin Levich Institute for Physico-Chemical Hydrodynamics and Department of Chemical Engineering, City College of New York, CUNY, 1-M Steinman Hall, 140th Street at Convent Avenue, New York, NY 10031, USA

Received 11 March 2003; received in revised form 12 July 2003

Abstract

Inertialess planar contraction flow with a Navier (linear) slip boundary condition has been studied for Newtonian and inelastic non-Newtonian fluids. For Newtonian fluids there is a region of curved streamlines as the flow adjusts from an upstream no-slip region with radial streamlines to a downstream slip-flow region that also has radial streamlines. Power-law fluids exhibit qualitatively different transverse flows for $n > 0.5$ and $n < 0.5$, with radial flow for $n = 0.5$; it is the *downstream* flow that approaches no-slip for $n < 0.5$, while the upstream approaches slip flow. Carreau–Yasuda fluids show a transition from Newtonian behavior upstream to power-law behavior downstream. The most interesting case is a Carreau–Yasuda fluid with $n < 0.5$, where the azimuthal velocity changes direction, causing significant curvature in the streamlines. The streamline curvature may be relevant to the onset of entry flow instabilities at high stress levels in polymer processing.

Keywords: Slip; Converging flow; Contraction; Boundary conditions; Streamline curvature; Carreau–Yasuda fluid

1. Introduction

Converging flow through a circular or planar channel is a common feature in polymer processing operations. Analytical solutions for planar contraction flow of inelastic and weakly viscoelastic fluids employing the no-slip boundary condition are well known; inelastic liquids follow radial streamlines, while weakly viscoelastic liquids may exhibit a small secondary flow very close to the exit [1–4]. Stress levels in polymer processing operations are often sufficiently high, however, that the fluid exhibits apparent slip at the solid boundary [5]. Flow with perfect slip will be radial for all constitutive equations.

In this paper, we analyze the creeping flow of Newtonian and inelastic non-Newtonian fluids in a planar contraction with a Navier (linear) slip boundary condition. We find that curved streamlines arise in the presence of wall slip, which may be a factor in the initiation of instabilities associated with entry flows.

* Corresponding author. fax: +1-212-650-6835.
E-mail address: denn@ccny.cuny.edu (M.M. Denn).

0377-0257/$ – see front matter © 2003 Elsevier B.V. All rights reserved.
doi:10.1016/S0377-0257(03)00151-4

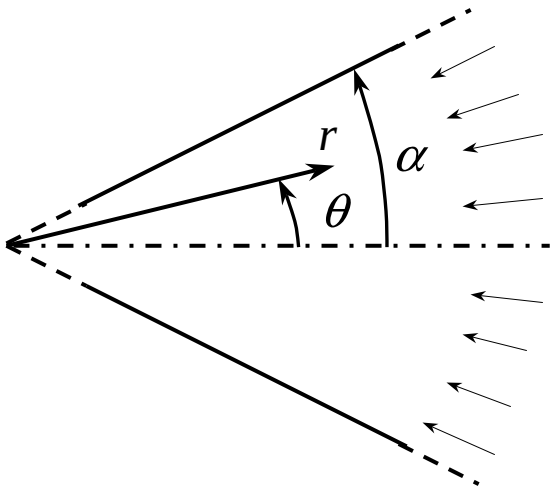

Fig. 1. Planar converging flow.

2. Newtonian fluid

We consider the planar contraction geometry shown in Fig. 1. The radial coordinate is measured from the vertex where the plates nominally meet, and the total angle between the two planes is 2α, with walls at $\theta = \pm\alpha$. The two-dimensional creeping flow equations for an incompressible Newtonian fluid can be written in terms of the stream function as

$$\nabla^4 \bar{\psi} = 0. \tag{1}$$

The radial and azimuthal components of velocity, $\bar{v}_r$ and $\bar{v}_\theta$, are then

$$\bar{v}_r = \frac{1}{r}\frac{\partial \bar{\psi}}{\partial \theta}, \qquad \bar{v}_\theta = -\frac{\partial \bar{\psi}}{\partial r}. \tag{2}$$

The solutions to Eq. (1) with boundary conditions of either no-slip or no-tangential stress exhibit radial flow profiles. We consider here a Navier slip boundary condition at the plates,

$$\bar{v}_r = \mp\beta\sigma_{r\theta}, \quad \text{at}\,\theta = \pm\alpha, \tag{3a}$$

where β is a constant that is characteristic of the fluid/solid pair. Incorporating the Newtonian fluid constitutive equation, the boundary condition becomes

$$\bar{v}_r = \mp\beta\eta\left[\frac{\partial \bar{v}_\theta}{\partial r} - \frac{\bar{v}_\theta}{r} + \frac{1}{r}\frac{\partial \bar{v}_r}{\partial \theta}\right] \quad \text{at}\,\theta = \pm\alpha. \tag{3b}$$

The condition of no flow through the walls requires

$$\bar{v}_\theta = 0 \quad \text{at}\,\theta = \pm\alpha. \tag{4}$$

Eq. (3b) can be written in terms of the stream function as

$$\frac{\partial \bar{\psi}}{\partial \theta} = \mp\left(\frac{\beta\eta}{r}\right)\left(\frac{\partial^2 \bar{\psi}}{\partial \theta^2} - r^2\frac{\partial^2 \bar{\psi}}{\partial r^2}\right) \quad \text{at}\,\theta = \pm\alpha. \tag{5a}$$

We now make use of the following dimensionless variables:

$$\Re = \frac{r}{\beta\eta}, \quad \psi = \frac{2\alpha\bar{\psi}}{q}, \quad \phi = \frac{\theta}{\alpha} \quad \text{and} \quad \boldsymbol{v} = \frac{2\alpha\beta\eta}{q}\bar{\boldsymbol{v}}.$$

Here, q is the flow rate per unit width, which is negative for converging flow. Eq. (5a) then becomes

$$\frac{\partial\psi}{\partial\phi} = \mp\Re^{-1}\alpha^{-1}\left(\frac{\partial^2\psi}{\partial\phi^2} - \Re^2\alpha^2\frac{\partial^2\psi}{\partial\Re^2}\right) \quad \text{at } \phi = \pm 1. \tag{5b}$$

The product $\beta\eta$ is the de Gennes slip extrapolation length [6], which is of molecular scale for polymer melts at low stresses but can be of the order of millimeters at high stresses, especially in the presence of fluoropolymer additives [7]. We recover the no-slip boundary condition as $\Re \to \infty$, while we recover the no-tangential stress (complete slip) boundary condition as $\Re \to 0$. With this observation we can anticipate the form of the solution for the Newtonian liquid: We expect radial flow far from the vertex (no slip) and also close to the vertex (no stress), with an intermediate transition region. The flow in the transition region will slow down at the center plane and speed up at the wall, so there must be an azimuthal velocity directed away from the center plane to maintain continuity. (A dimensionless velocity away from the center plane is negative for $0 < \phi < 1$.)

It is straightforward to obtain regular perturbation solutions valid for $\Re \ll 1$ and $\Re \gg 1$. We first consider the case $\Re \ll 1$, for which the base case is the radial flow associated with the no-stress boundary condition. We write the stream function as $\psi = \psi^0 + \Re\psi^1 + \mathrm{O}(\Re^2)$. $\psi^0 = \alpha\phi$ is the complete solution

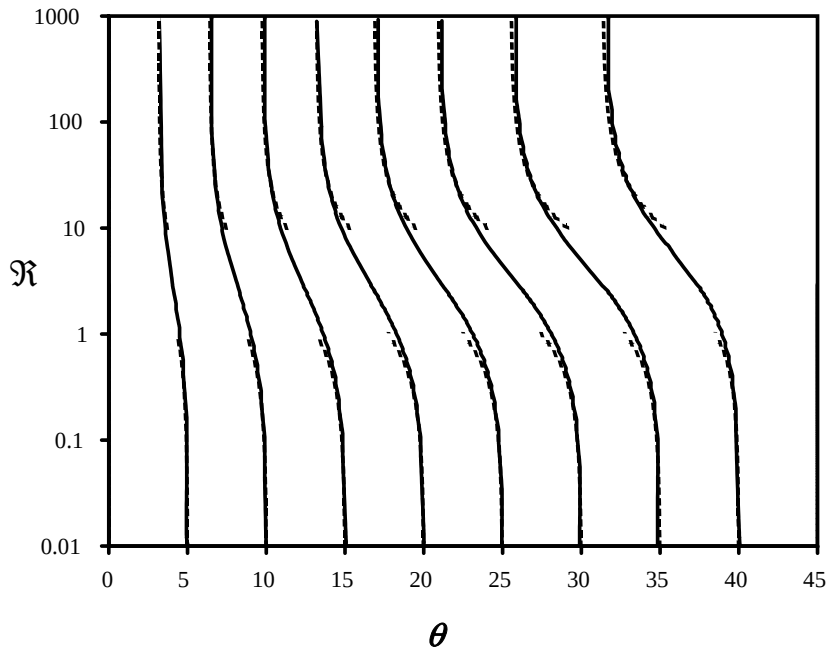

Fig. 2. Streamlines for a Newtonian fluid. The solid lines are the finite-element solution, while the broken lines are the first-order perturbation solutions.

for the no stress boundary condition, while the general expression for ψ^1 is $\psi^1 = a_1 \sin\alpha\phi + b_1 \cos\alpha\phi + \bar{a}\phi \sin\alpha\phi + \bar{b}\phi \cos\alpha\phi$. After satisfying the boundary conditions we obtain

$$\psi = \alpha\phi + \Re\left(\frac{\alpha}{2\sin\alpha}\phi\cos\alpha\phi - \frac{\alpha}{2\tan\alpha\sin\alpha}\sin\alpha\phi\right) + \mathrm{O}(\Re^2). \tag{6}$$

For $\Re \gg 1$, we expand in $\Re^{-1}$, for which the base case is the radial flow associated with no slip. We write the stream function as $\psi = \psi^0 + \Re^{-1}\psi^1 + \mathrm{O}(\Re^{-2})$. $\psi^0 = a_0\phi + b_0 \sin 2\alpha\phi$ satisfies the no-slip boundary condition. The general expression for ψ^1 is $\psi^1 = a_1 \sin\alpha\phi + b_1 \cos\alpha\phi + a_3 \sin 3\alpha\phi + b_3 \cos 3\alpha\phi$. After satisfying the boundary conditions we obtain

$$\psi = \frac{2\alpha}{\tan 2\alpha - 2\alpha}\left(\frac{\sin 2\alpha\phi}{2\cos 2\alpha} - \alpha\phi\right) + \Re^{-1}\left[\frac{-4\alpha\tan 2\alpha}{(\tan 2\alpha - 2\alpha)\,(\tan 3\alpha - 3\tan\alpha)}\left(\frac{\tan 3\alpha}{\cos\alpha}\sin\alpha\phi - \frac{\tan\alpha}{\cos 3\alpha}\sin 3\alpha\phi\right)\right] + \mathrm{O}(\Re^{-2}). \tag{7}$$

The dimensionless streamlines from the perturbation solution are shown in Fig. 2 for $\alpha = \pi/4$, together with streamlines computed using the finite-element code POLYFLOW^{TM}. The finite-element solution was obtained by systematically changing the spatial region in order to obtain results over five orders of magnitude in $\Re$. The numerical solution appears to exhibit small inaccuracies, hence the slight deviation from the asymptotic solution for very large $\Re$. The perturbation solutions are

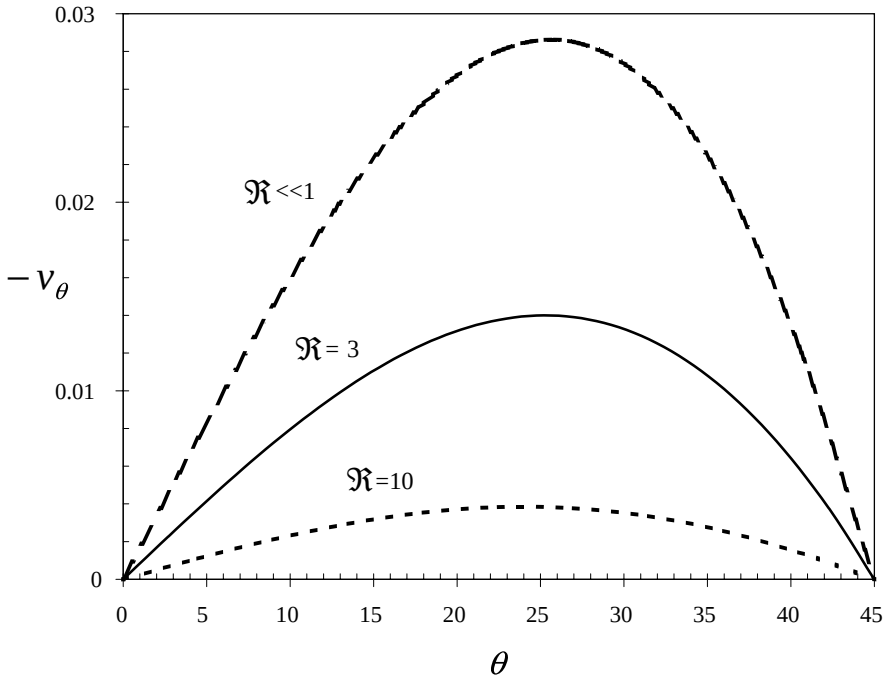

Fig. 3. Azimuthal component of the velocity at various locations for a Newtonian fluid. Dashed and dotted lines are the perturbation solutions. The solid line is a finite-element solution at an intermediate position.

reasonably accurate for $\Re < 1$ and $\Re > 10$. The expected streamline curvature is clearly seen, with the transition starting at radial positions one to two orders of magnitude greater than the slip length.

The dimensionless azimuthal velocity v_θ is shown in Fig. 3. The values for $\Re \ll 1$ and $\Re = 10$ are computed from the perturbation solutions, while the value for $\Re = 3$ is from the finite-element solution. v_θ is independent of $\Re$ in the region where the linear expansion in $\Re$ for the stream function is valid. The flow is away from the center plane and towards the wall, as expected.

3. Power-law fluid

The viscosity for a power-law fluid is given by

$$\eta = K\dot{\gamma}^{n-1}, \tag{8}$$

where $\dot{\gamma} = \sqrt{(1/2)\mathrm{II}}$ for a general flow; $\mathrm{II} = \boldsymbol{\kappa} : \boldsymbol{\kappa}$ is the second invariant of the deformation rate tensor $\boldsymbol{\kappa}$. Non-dimensionalization now leads to a dimensionless length scale $\tilde{\Re} = (2\alpha)^{n-1}r^{2n-1})/\beta K|q|^{n-1}$, which still has the physical meaning of the ratio of radial position to slip length. The case $n = 0.5$ is of special interest, in that the dimensionless length scale $\tilde{\Re}$ is independent of radius, implying that the stream function is independent of r. We seek a solution for this case with $\bar{v}_\theta = 0$, for which the continuity equation requires the radial component of velocity to have the form

$$\bar{v}_r = \frac{f(\theta)}{r}. \tag{9}$$

The details of the solution method are given in Appendix A. $F = \alpha f/q$ is a function of the reduced angle $\phi = \theta/\alpha$ and the single parameter $\tilde{\Re}$. Fig. 4 shows F as a function of θ for $\alpha = \pi/4$ and various values of $\tilde{\Re}$. As expected, the solution tends towards plug flow with decreasing $\tilde{\Re}$.

The case $n = 0.5$ represents an important transition. For $1 \geq n > 0.5$, the azimuthal flow is away from the center plane, consistent with a transition from no-slip as $r \to \infty$ to complete slip as $r \to 0$. For $n = 0.5$, the azimuthal flow vanishes, indicating that the boundary behavior is the same for all values of r. Fig. 5 shows streamlines computed using POLYFLOW^{TM} for $n = 0.3$; the dashed lines for small r (large $\tilde{\Re}$, since $\tilde{\Re} \sim r^{-0.4}$) show the fully-developed solution with a no-slip boundary condition, while the dashed lines for large r (small $\tilde{\Re}$) are a first-order perturbation solution[1] in $\tilde{\Re}$ about the solution for perfect slip. Hence, for $0 < n < 0.5$, the azimuthal flow is *towards* the center plane, with a transition from perfect slip as $r \to \infty$ to no-slip as $r \to 0$. This counterintuitive behavior is consistent with the

[1] It is straightforward to show that $\tilde{\Re}$ is the appropriate expansion variable about the radial solution with no tangential stress and $\tilde{\Re}^{-1}$ is the appropriate expansion variable about the radial no-slip solution. A closed-form solution for the latter is not available. The expansion in $\tilde{\Re}$ for any n is as follows:

$$1 > n > 0.5: \quad \psi = \alpha\phi + \tilde{\Re}\left(\frac{2^{1-n}}{(\xi^2-1)\sin\xi\alpha}\sin\xi\alpha\phi - \frac{2^{1-n}}{(\xi^2-1)\sin\alpha}\sin\alpha\phi\right) + \mathrm{O}(\tilde{\Re}^2),$$

$$0.5 > n > 0: \quad \psi = \alpha\phi + \tilde{\Re}\left(\frac{2^{1-n}}{(\xi^2-1)\sin\alpha}\sin\alpha\phi - \frac{2^{1-n}}{(\xi^2-1)\sinh\xi\alpha}\sinh\xi\alpha\phi\right) + \mathrm{O}(\tilde{\Re}^2).$$

Here, $\xi = \sqrt{|(1-2n)(3-2n)|}$.

observation that $\tilde{\Re}$ is the appropriate dimensionless length scale, since $\tilde{\Re} \to \infty$ (0) corresponds to either $\beta \to 0$ (∞) or $r \to 0$ (∞).

We can gain some insight into this unusual behavior by considering rectilinear shear flow of a power-law fluid through a plane slit with gap H, with a Navier slip boundary condition at both faces ($y = 0$ and H).

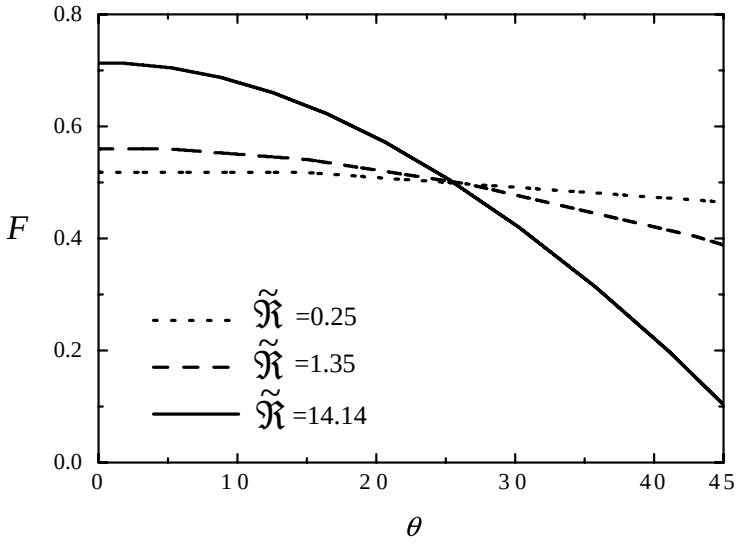

Fig. 4. F as a function of θ for various values of $\tilde{\Re}$ for a power-law fluid with $n = 0.5$.

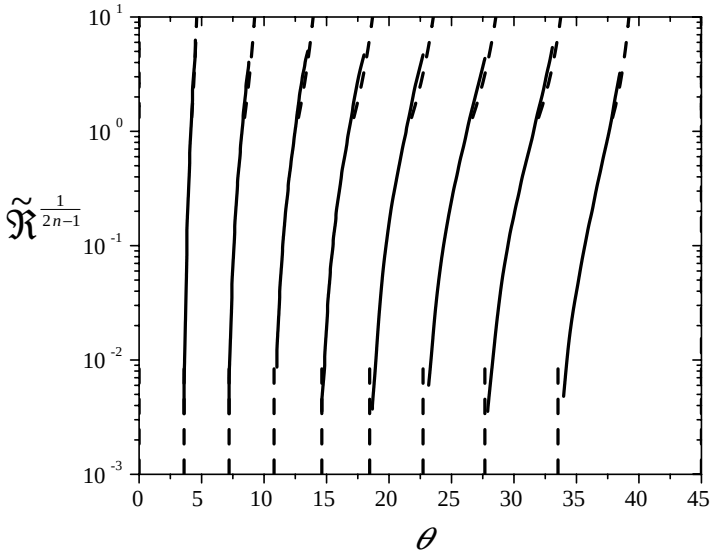

Fig. 5. Streamlines for a power-law fluid with $n = 0.3$. The dashed lines in the upstream region represent the perturbation solution around the no-stress boundary condition, while the dashed lines downstream represent the solution for a no-slip boundary condition.

For $\bar{v}_x = \bar{v}_x(y)$ and $\bar{v}_y = 0$, the flow rate per unit width is

$$q = \frac{nH^2}{2(2n+1)} \left(\frac{H}{2K} \left| \frac{\mathrm{d}P}{\mathrm{d}x} \right| \right)^{1/n} + \beta \frac{H^2}{4} \left| \frac{\mathrm{d}P}{\mathrm{d}x} \right|, \tag{10}$$

and the slip velocity is given by

$$\bar{v}_s = \bar{v}_x|_{y=0} = \beta \frac{H}{2} \left| \frac{\mathrm{d}P}{\mathrm{d}x} \right|. \tag{11}$$

From Eqs. (10) and (11), we can write q in terms of $\bar{v}_s$ as

$$q = \frac{nH^2}{2(2n+1)} \left(\frac{\bar{v}_s}{\beta K} \right)^{1/n} + \frac{H}{2} \bar{v}_s. \tag{12}$$

We now think in terms of the lubrication approximation for small α, where $H \sim r\alpha$, and treat Eq. (12) as an equation for the slip velocity. It is straightforward to show for $n > 0.5$ that the first term on the right determines $\bar{v}_s$ for $r \to \infty$, while the second term on the right determines $\bar{v}_s$ for $r \to 0$; this is consistent with the understanding gained from the Newtonian fluid, where the upstream flow approaches the no-slip asymptote while the downstream flow approaches the full slip asymptote. For $n < 0.5$, however, the situation is reversed, and the first term on the right determines $\bar{v}_s$ for $r \to 0$, while the second term determines $\bar{v}_s$ for $r \to \infty$. This is consistent with the observations from the POLYFLOW™ simulations and the perturbation solution.

3.1. Carreau–Yasuda (C–Y) model

The viscosity function in the Carreau–Yasuda (C–Y) model is given by

$$\eta = \eta_0 [1 + (\lambda \dot{\gamma})^a]^{(n-1)/a}. \tag{13}$$

The C–Y equation is more realistic for real polymer melts than the power law, because it approaches a Newtonian zero-shear viscosity at small deformation rates and power-law behavior at large deformation rates. We intuitively expect Newtonian fluid behavior for large r and power-law behavior for small r; based on the results in the two preceding sections we might therefore anticipate unusual streamlines for $n < 0.5$. The C–Y fluid will begin to show marked deviation from Newtonian behavior for $\lambda \dot{\gamma} \approx 1$. The characteristic deformation rate $\dot{\gamma}$ for the converging geometry is of the order of

$$\dot{\gamma} \approx \frac{q}{2\,(\alpha r)^2}. \tag{14}$$

We use the Newtonian fluid non-dimensionalization, $r = \Re \beta \eta_0$, in which case we expect deviation from Newtonian behavior for $\Re^2 \approx w$, where w is defined as

$$w = \frac{q\lambda}{2\,(\alpha\beta\eta_0)^2}. \tag{15}$$

Fig. 6 shows streamlines obtained from the POLYFLOW™ simulation for a C–Y fluid with $w = 4.0$ and $n = 0.3$. The streamlines for the C–Y and Newtonian fluids are identical for $\Re \gg \sqrt{w}$, while the C–Y fluid merges into the power-law fluid with $n = 0.3$ for $\Re \ll \sqrt{w}$. The azimuthal flow is away from the center plane for $\Re > \sqrt{w}$ and towards the center plane for $\Re < \sqrt{w}$.

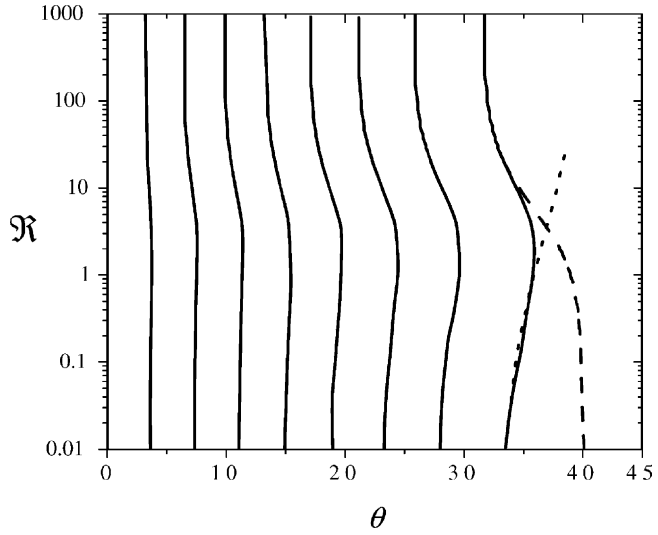

Fig. 6. Streamlines for a Carreau–Yasuda fluid with $n = 0.3$ and $w = 4.0$. The dashed line is the streamline for a Newtonian fluid ($w = 0$), while the dotted line is the streamline for the corresponding power-law fluid.

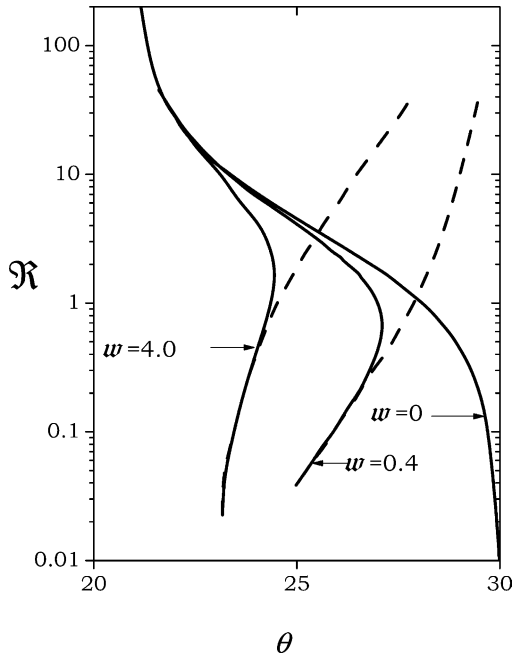

Fig. 7. A streamline for a Carreau–Yasuda fluid with $n = 0.3$ for various values of w; the Newtonian fluid is $w = 0$. The dashed lines are the corresponding power-law streamlines.

Fig. 7 shows a single streamline for a Carreau–Yasuda fluid with $n = 0.3$ for various values of w. The two broken lines denoting the power-law fluid do not overlap because of the use of the length scaling based on the zero-shear viscosity. The maximum deviation from the upstream no-slip Newtonian flow and downstream no-slip C–Y flow occurs for $\Re \approx \sqrt{w}$, where the azimuthal velocity changes direction.

4. Conclusion

Power-law behavior with wall slip, in which the azimuthal velocity reverses direction and the asymptotic behavior changes from slip to no-slip as n passes through 0.5, is relevant to most polymer processing applications only in the downstream region because of the unphysical behavior of the power-law viscosity as the deformation rate goes to zero. The Carreau–Yasuda fluid, however, which is more realistic for real polymer melts, also shows very interesting and unexpected behavior. The most important case is the Carreau–Yasuda fluid with $n < 0.5$, where the azimuthal velocity changes direction within the flow field at $\Re \approx \sqrt{w}$ and there is substantial curvature in the streamlines.

We believe this result is of some significance, because the slip at the boundary at high stresses may be related to the entry flow instability that is often observed in polymer melts and is believed by many investigators to be the "trigger" for gross melt fracture [8]. While we have dealt here only with inelastic constitutive equations, viscoelastic constitutive equations should lead to flow fields that are at least as complex in converging geometries with wall slip. The presence of curved streamlines is generally believed to provide the initiating mechanism for viscoelastic instabilities at low Reynolds numbers [9,10].

Acknowledgements

We are grateful to Prof. Andreas Acrivos for help with the perturbation solution, and to an anonymous reviewer for asking pertinent questions that led to a substantially improved manuscript.

Appendix A. Power-law fluid with $n = 0.5$

We seek a radial solution, in which case

$$\bar{v}_r = \frac{f(\theta)}{r}. \tag{A.1}$$

Writing the Cauchy momentum equations for creeping flow in the r and θ directions and eliminating the pressure term, we obtain a second order partial differential equation for the stress:

$$\frac{\partial^2(\sigma_{rr} - \sigma_{\theta\theta})}{\partial\theta\partial r} + \frac{1}{r}\frac{\partial(\sigma_{rr} - \sigma_{\theta\theta})}{\partial\theta} + \frac{1}{r}\frac{\partial^2\sigma_{r\theta}}{\partial\theta^2} - r\frac{\partial^2\sigma_{r\theta}}{\partial r^2} - 3\frac{\partial\sigma_{r\theta}}{\partial r} = 0. \tag{A.2}$$

For radial flow of a power-law fluid, the second invariant term in the viscosity becomes

$$\left|\frac{1}{2}\mathrm{II}\right|^{(n-1)/2} = \frac{\left(4f^2 + (f')^2\right)^{(n-1)/2}}{r^{2(n-1)}} = \frac{g(\theta)}{r^{2(n-1)}}, \tag{A.3}$$

where $f' = \mathrm{d}f/\mathrm{d}\theta$ and $g(\theta) = (4f^2 + (f')^2)^{(n-1)/2}$. The viscosity is then given by

$$\eta = \frac{Kg(\theta)}{r^{2(n-1)}}. \tag{A.4}$$

The components of the stress tensor are

$$\sigma_{rr} = -\frac{2Kgf}{r^{2n}}, \quad \sigma_{\theta\theta} = \frac{2Kgf}{r^{2n}} \quad \text{and} \quad \sigma_{r\theta} = \frac{2Kgf'}{r^{2n}}, \tag{A.5}$$

and Eq. (A.2) reduces to an ordinary differential equation,

$$\frac{\mathrm{d}^2(gf')}{\mathrm{d}\theta^2} + gf' = 0. \tag{A.6}$$

Defining $F = \alpha f/q$, a solution to Eq. (A.6) can be written in dimensionless form for the specific case of $n = 0.5$ as

$$\left(4F^2 + (F')^2\right)^{-0.25} F' = c_1 \cos\alpha\phi + c_2 \sin\alpha\phi. \tag{A.7}$$

Similarly, the Navier boundary condition can be written as

$$\tilde{\Re} F = \mp\sqrt{2}\left(4F^2 + (F')^2\right)^{-0.25} F' \quad \text{at } \phi = \pm 1. \tag{A.8}$$

where $\tilde{\Re} = |q|^{0.5}/\sqrt{2\alpha}\beta K$ for $n = 0.5$. (The independence of $\tilde{\Re}$ on r is what permits a radial solution for $n = 0.5$.) We further require that

$$\int_{-1}^{1} F\,\mathrm{d}\phi = 1. \tag{A.9}$$

In order to solve Eq. (A.7), we take $F = F_{\mathrm{cl}}\Theta$, where F_{cl} is the value of F at $\phi = 0$ (hence $\Theta = 1$ at $\phi = 0$). We can then write Eq. (A.7) as

$$\Theta' = c_3 \sin\alpha\phi \left(4\Theta^2 + (\Theta')^2\right)^{0.25}, \tag{A.10}$$

and

$$F_{\mathrm{cl}} = \frac{0.5}{\int_0^1 \Theta\,\mathrm{d}\phi}, \tag{A.11}$$

with

$$\sqrt{2}\Theta' = -F_{\mathrm{cl}}\tilde{\Re}\Theta\left(4\Theta^2 + (\Theta')^2\right)^{0.25} \quad \text{at } \phi = 1. \tag{A.12}$$

We now specify c_3 and solve Eq. (A.10) numerically for $\Theta(\phi)$. The corresponding values of F_{cl} and $\tilde{\Re}$ are then calculated using Eqs. (A.11) and (A.12), respectively, providing a one-parameter family of solutions as c_3 is varied.

References

[1] J.R. Black, M.M. Denn, Converging flow of a viscoelastic liquid, J. Non-Newtonian Fluid Mech. 1 (1976) 83–92.

[2] J.R. Black, M.M. Denn, G.C. Hsiao, in: J.F. Hutton, J.R.A. Pearson, K. Walters (Eds.), Theoretical Rheology, Applied Science, London, 1975, pp. 3–30.
[3] K. Strauss, in: J.F. Hutton, J.R.A. Pearson, K. Walters (Eds.), Theoretical Rheology, Applied Science, London, 1975, pp. 56–66.
[4] M.M. Denn, Process Fluid Mechanics, Prentice-Hall, New York, 1980.
[5] M.M. Denn, Extrusion instabilities and wall slip, Annu. Rev. Fluid Mech. 33 (2001) 265–287.
[6] P.G. de Gennes, Ecoulements viscometriques de polymers enchevetres, C.R. Acad. Sci. Paris, Ser. B 288 (1979) 219–220.
[7] X. Yang, H. Ishida, S.Q. Wang, Wall slip and absence of interfacial flow instabilities in capillary flow of various polymer melts, J. Rheol. 42 (1998) 63–80.
[8] C.J.S. Petrie, M.M. Denn, Instabilities in polymer processing (Journal Review), AIChE J. 22 (1976) 209–236.
[9] G.H. McKinley, P. Pakdel, A. Öztekin, Rheological and geometric scaling of purely elastic flow instabilities, J. Non-Newtonian Fluid Mech. 67 (1996) 19–47.
[10] E.S.G. Shaqfeh, Purely elastic instabilities in viscometric flows, Annu. Rev. Fluid Mech. 28 (1996) 129–185.